Journal of Magnetic Resonance 251 (2015) 52–56

Contents lists available at ScienceDirect

Journal of Magnetic Resonance

journal homepage: www.elsevier.com/locate/jmr

Communication

Two heteronuclear dipolar results at the price of one: Quantifying Na/P contacts in phosphosilicate glasses and biomimetic hydroxy-apatite

Baltzar Stevensson, Renny Mathew, Yang Yu, Mattias Edén *

Physical Chemistry Division, Department of Materials and Environmental Chemistry, Arrhenius Laboratory, Stockholm University, SE-106 91 Stockholm, Sweden

ARTICLE INFO

Article history:
Received 27 October 2014
Revised 1 December 2014
Available online 17 December 2014

Keywords:
Heteronuclear dipolar recoupling
^{23}Na{^{31}P} REDOR
^{31}P{^{23}Na} REAPDOR
Silicate glasses
Molecular dynamics simulations

ABSTRACT

The analysis of S{I} recoupling experiments applied to amorphous solids yields a heteronuclear second moment M_2(S–I) that represents the effective through-space dipolar interaction between the detected S spins and the neighboring I-spin species. We show that both M_2(S–I) and M_2(I–S) values are readily accessible from a sole S{I} or I{S} experiment, which may involve either S or I detection, and is naturally selected as the most favorable option under the given experimental conditions. For the common case where I has half-integer spin, an I{S} REDOR implementation is preferred to the S{I} REAPDOR counterpart. We verify the procedure by ^{23}Na{^{31}P} REDOR and ^{31}P{^{23}Na} REAPDOR NMR applied to Na_2O–CaO–SiO_2–P_2O_5 glasses and biomimetic hydroxyapatite, where the M_2(P–Na) values directly determined by REAPDOR agree very well with those derived from the corresponding M_2(Na–P) results measured by REDOR. Moreover, we show that dipolar second moments are readily extracted from the REAPDOR NMR protocol by a straightforward numerical fitting of the initial dephasing data, in direct analogy with the well-established procedure to determine M_2(S–I) values from REDOR NMR experiments applied to amorphous materials; this avoids the problems with time-consuming numerically exact simulations whose accuracy is limited for describing the dynamics of *a priori* unknown multi-spin systems in disordered structures.

1. Introduction

Heteronuclear dipolar recoupling for determining internuclear distances in spin-1/2 pairs undergoing magic-angle-spinning (MAS) is a well-developed area [1–3]. Notably, the rotational echo double resonance (REDOR) [4] protocol is one of the most widely applied techniques in solid state NMR. S{I} REDOR reintroduces the S–I through-space dipolar interactions by application of two π-pulses per rotational period ($\tau_r = \nu_r^{-1}$, where ν_r is the MAS frequency in Hz) to either the detected S-spin species, or to its coupled I-spin partner(s). Transverse S-spin magnetization thereby evolves for a controlled recoupling period $\tau_{rec} = 2n\tau_r$ ($n = 1, 2, 3, \ldots$), leading to an attenuated ("dipolar dephased") NMR signal $[S(\tau_{rec})]$ relative to a reference counterpart $[S_0(\tau_{rec})]$ obtained by a spin-echo [4]. Fitting of the $\Delta S/S_0 \equiv [S_0(\tau_{rec}) - S(\tau_{rec})]/S_0(\tau_{rec})$ "dephasing curve" to numerical simulations or an analytical solution [5], allows extraction of the S–I dipolar coupling constant $b_{S-I} = b_{I-S} = -\mu_0\hbar\gamma_S\gamma_I/(8\pi^2 r_{S-I}^3)$. Alternatively, for large S_mI_n multi-spin systems where determinations of individual S–I distances are often intractable, fitting of the *initial* dephasing data $\Delta S/S_0 \lesssim 0.2$ to a parabolic relationship $\sim M_2(\text{S—I})\tau_{rec}^2$ [1,6–8], yields an estimation of the van Vleck *dipolar second moment* [9],

$$M_2(\text{S—I}) = \frac{4}{15} I(I+1) N_S^{-1} \sum_j^{N_S} \sum_k^{N_I} \left(b_{S-I}^{jk}\right)^2, \quad [\text{unit}: \ s^{-2} = Hz^2], \quad (1a)$$

$$M_2(\text{I—S}) = \frac{4}{15} S(S+1) N_I^{-1} \sum_k^{N_I} \sum_j^{N_S} \left(b_{I-S}^{kj}\right)^2, \quad (1b)$$

where N_I and N_S represent the respective numbers of I and S sites in the structure, while I and S denote the spin quantum numbers. Note the very similar expressions for M_2(S—I) and M_2(I—S), as well as that $b_{S-I}^{jk} \equiv b_{I-S}^{kj}$.

Dipolar recoupling involving an $S = 1/2$ and a quadrupolar $I > 1/2$ nucleus is significantly more challenging due to the problems of simultaneously arranging efficient dephasing of all I-spin single-quantum transitions [10,11]. Several options are proposed [1,10–18]. The most commonly utilized protocol, rotational echo adiabatic passage double resonance (REAPDOR; [10,11]), extends an existing REDOR implementation in that all π-pulses are applied to the spin-1/2 (S) species but the central π-pulse of the I-spin channel is replaced by a strong "adiabatic passage" (AP) pulse

* Corresponding author.
E-mail address: mattias.eden@mmk.su.se (M. Edén).

http://dx.doi.org/10.1016/j.jmr.2014.12.002
1090-7807/

lasting for $\sim \tau_r/3$ [10,11]. To achieve efficient dipolar recoupling without a pronounced dependence on the quadrupolar tensor parameters, the experimental conditions should for $I = 3/2$ obey the "adiabaticity requirement" $\alpha \equiv 2\nu_1^2/(\nu_r C_Q) \gtrsim 0.5$ [11], where ν_1 is the rf nutation frequency and $C_Q = e^2qQ/h$ the quadrupolar coupling constant.

Two main hurdles complicate S{I} REAPDOR applications for estimating b_{S-I} or M_2(S—I) data: (*i*) To obey the adiabaticity condition for large quadrupolar couplings, very strong rf powers are generally required (that may be intractable) and/or the MAS rate must be limited, which inflicts a coarser sampling of the recoupling dynamics because $\Delta\tau_{rec} = 2\tau_r$. These problems may be mitigated by modified experimental protocols where the AP rf pulse is replaced by a longer but less rf power-demanding pulse [14,16–18]. (*ii*) As opposed to the REDOR dephasing that is analytically solvable [5], the extraction of internuclear-distance related information from the more complex REAPDOR dynamics has traditionally involved numerically exact simulations. If the AP pulse is truly adiabatic, it has been demonstrated for S–I *spin-pairs* that the REAPDOR NMR data may be fitted to an empirically deduced "universal curve" [11,19,20]. However, its application for extracting internuclear distances or M_2(S—I) values from *multi-spin* systems remains to our knowledge unexplored, particularly for disordered network structures where even numerically exact calculations may lack accuracy because the NMR parameters exhibit *a priori* unknown distributions, while the simulated spin-system size must naturally be restricted to avoid prohibitive computation times. Herein, we demonstrate that M_2(S—I) values are *directly* accessible by fitting experimental S{I} REAPDOR NMR data either to the "universal curve" [20], or to a truncated Taylor expansion (TE) of an analytical S–I two-spin solution [5] in the limit $M_2(\text{S—I})\tau_{rec} \ll 1$; the latter approach prevails REDOR analyses in amorphous materials [1,6–8].

However,given the complications associated with M_2(S—I) estimates from REAPDOR experimentation on SI_n systems in disordered structures—and heteronuclear dipolar recoupling involving non-negligible rf application to quadrupolar nuclei *vide infra*—we here propose a pragmatic solution: whenever feasible, *avoid* the S{I} ($S = 1/2$; $I > 1/2$) experiment *altogether* and instead derive the M_2(S—I) value from its counterpart M_2(I—S) determined from an I{S} protocol such as REDOR. Provided that the I-spin MAS NMR spectrum is readily detected and its signals are not severely broadened by second-order quadrupolar interactions such that the central-transition (CT) magnetization may be accurately inverted by a CT-selective π-pulse, all dipolar recoupling pulses are applied to the (now non-observed) $S = 1/2$ species. The dipolar dephasing is analyzed by a straightforward data fitting [1,6,8]. Next, for known molar fractions x_I and x_S of the I and S species in the sample, respectively, the M_2(S—I) value may be derived from the simple relationship

$$M_2(\text{S—I}) = \frac{f_I x_I I(I+1)}{f_S x_S S(S+1)} M_2(\text{I—S}), \tag{2}$$

where f_I and f_S represent the corresponding isotope abundances. Eq. (2) follows directly by combining Eqs. (1a) and (1b), where each product $f_I x_I$ and $f_S x_S$ corresponds to N_I and N_S, respectively.

Consequently, *both* M_2(S—I) and M_2(I—S) values are accessible from *one* single S{I} *or* I{S} recoupling experiment, naturally selected as the most favorable option and usually constituting that of I{S}. In the contexts of Na_2O–CaO–SiO_2–P_2O_5 glasses and biomimetic hydroxyapatite grown *in vitro* at the surface of a mesoporous bioactive glass, we exploit the high sensitivity and fast T_1 relaxation of ^{23}Na to estimate M_2(P—Na) values by feeding the corresponding ^{23}Na{^{31}P} REDOR-derived M_2(Na—P) results through Eq. (2).

2. Results and discussion

2.1. Phosphosilicate glasses

The set of melt-prepared phosphosilicate glasses used herein comprises SiO_2 (40–60 mol%), P_2O_5 (2–6 mol%), Na_2O (17–24 mol%) and CaO (22–32 mol%); see Table S1. The glass preparation schemes and experimental/computational procedures are described in the Supplementary Information (SI). Each glass constitutes a network of interconnected SiO_4 tetrahedra, whereas P exists predominantly as orthophosphate (PO_4^{3-}) groups occupying interstitial positions around the silicate network [21,22]. The ^{31}P/^{29}Si MAS NMR spectra and the underlying silicate and phosphate speciations were recently discussed [21,22].

Thanks to the high sensitivity and 100% natural abundance of both ^{23}Na and ^{31}P, ^{23}Na{^{31}P} REDOR as well as ^{31}P{^{23}Na} REAPDOR data were readily acquired from the glass series, although due to a slow ^{31}P T_1 relaxation and low amount of P in the present glasses, the REDOR NMR data collection is significantly faster than that of REAPDOR. The corresponding M_2(P—Na) and M_2(Na—P) values were extracted by fitting the initial dephasing regime ($\Delta S/S_0 \lesssim 0.1$) to a TE truncated at the second term, whereas the REAPDOR data-sets were also fitted to the "universal curve" of [20]. The SI provides detailed information about the analysis, together with plots of the experimental and best-fit dephasing curves.

Fig. 1a plots the REDOR-stemming best-fit M_2(Na—P) data (open circles) against the number density of P atoms (ρ_P) in the glass. The observed linear increase of M_2(Na—P) for growing ρ_P implies a continuously expanding number of Na^+–PO_4^{3-} contacts in the structure, thereby suggesting the absence of any pronounced preference for Na to partition around silicate and phosphate species (or weak trend thereof). The consequences of the observed composition-dependent trends of the Na/P contacts will be discussed in detail elsewhere; herein, we focus solely on demonstrating the $M_2(\text{S—I}) \leftrightarrow M_2(\text{I—S})$ interconversion [Eq. (2)].

To assess the data accuracy, dephasing curves were recorded from powders of Na_3PO_4 and NaH_2PO_4 under identical experimental conditions as for the glasses. This provided best-fits amounting to 69.7% and 68.3% of the respective theoretical M_2(Na—P) value of the known crystal structures. Our experimentation involved full rotors, which unfortunately emphasizes rf-inhomogeneity effects that are known to diminish the REDOR dephasing [7,23]. Similar tendencies were noted to affect analogous estimates of effective ^{31}P–^{31}P internuclear contacts by double-quantum ^{31}P MAS NMR experimentation on these phosphosilicate glass structures [22]. However, the rf (in)homogeneity is independent on the glass sample and its other NMR-parameters, and furthermore appears to be the primary source of systematic experimental errors. Consequently, the best-fit second moment from each glass was scaled by the net factor $[(0.697 + 0.683)/2]^{-1} = 1.449$. Fig. 1a evidences an excellent accordance between the corrected experimental M_2(Na—P) values (solid circles) and those calculated from the atomic coordinates of glass models generated from atomistic molecular dynamics (MD) simulations (open boxes). See Refs. [21,22] and the SI for further details on the MD simulations.

Fig. 1(b)–(d) presents the M_2(P—Na) data extracted from the glasses, obtained either from MD simulations or ^{31}P{^{23}Na} REAPDOR NMR experiments. The corresponding REDOR-derived results from Eq. (2) are also displayed, as obtained (b) *before* and (d) *after* correction of the experimental data. Note that the M_2(P—Na) values increase linearly with ρ_{Na}. The REAPDOR dephasing fits to the universal curve were corrected by utilizing results from Na_3PO_4 and the same "calibration" procedure as for the REDOR NMR experimentation; this provided the scaling factor $0.739^{-1} = 1.354$. Its close value to that obtained from REDOR gives

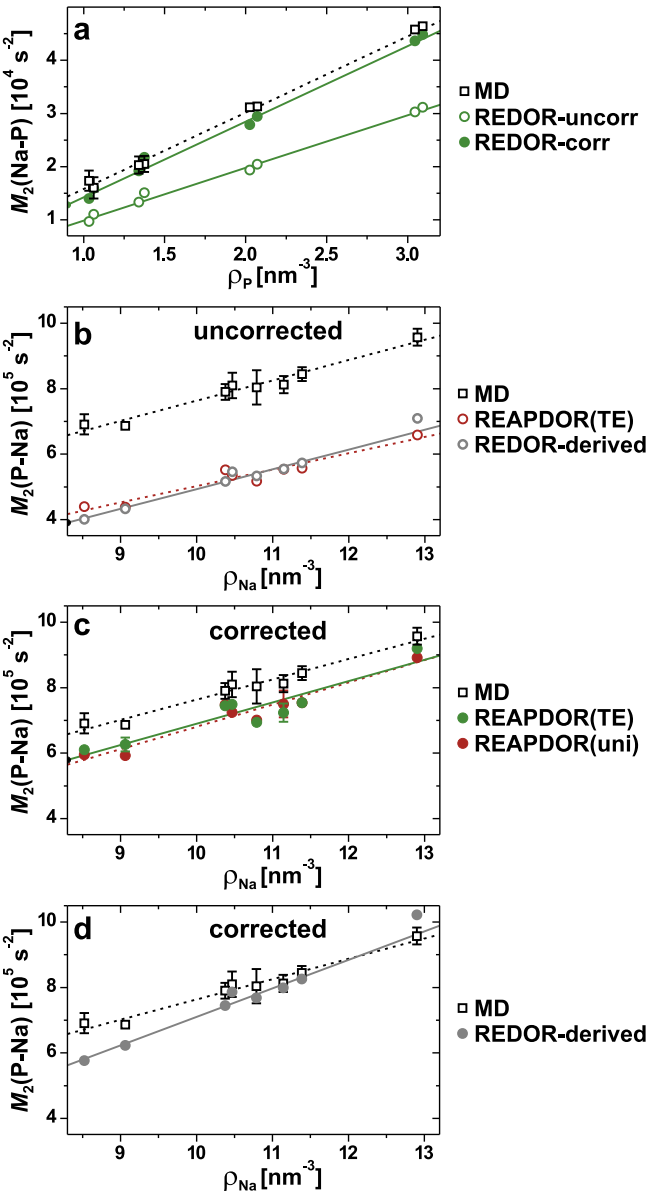

Fig. 1. Dipolar second moments obtained either from MD simulations or REDOR/REAPDOR NMR experiments, and plotted against the number density of (a) P or (b)–(d) Na in the Na_2O–CaO–SiO_2–P_2O_5 glass. (a) M_2(Na—P) values derived directly by numerical fitting of the initial regime of $^{23}Na\{^{31}P\}$ REDOR dephasing curves ("uncorr"), and after applying data correction ("corr"), as described in the text. (b)–(d) M_2(P—Na) results obtained either by (b, c) fitting of $^{31}P\{^{23}Na\}$ REAPDOR dephasing curves, or by converting the REDOR-derived data in (a) *via* Eq. (2), where (b) and (d) display the M_2(P—Na) estimates before and after correction, respectively. The labels "TE" and "uni" indicate that the experimental $^{31}P\{^{23}Na\}$ REAPDOR data was fitted to a Taylor expansion [Eq. (S1)] and the universal curve [Eq. (S2)], respectively. All REDOR data fitting involved the Taylor expansion. Error bars below the symbol sizes are not shown. All NMR results were recorded at 9.4 T and 14.0 kHz MAS rate by using full 4 mm zirconia rotors.

further support for our simplistic corrections. Figs. 1b and 1c show the respective (b) uncorrected and (c) corrected M_2(P—Na) data, notably evidencing an excellent consistency between the results stemming from each fitting approach, i.e., the universal curve or TE; see the SI for details.

It is particularly gratifying that the M_2(P—Na) values obtained indirectly by $^{23}Na\{^{31}P\}$ REDOR NMR manifest an overall very good agreement with their directly determined REAPDOR counterparts, regardless of whether the "uncorrected" or "corrected" pairs of data sets are compared. Fig. S2 plots the various independent M_2(P—Na) estimates against each other, revealing that the REDOR-derived values are generally ≈10% higher than their directly determined counterparts from REAPDOR (see the SI). Moreover, the REDOR data in conjunction with Eq. (2) evidences an even *better* agreement with the MD-generated M_2(P—Na) values (Fig. 1d) relative to those estimated directly from REAPDOR. Altogether, Fig. 1 provides a mutual validation of the NMR/MD results (where we have previously observed an overall very good accordance between other structural parameters [21,22]), as well as experimentally successful M_2(S—I) → M_2(I—S) interconversions.

2.2. Na substitution in biomimetic apatite

Most of the Na_2O–CaO–SiO_2–P_2O_5 glasses examined above are *bioactive* [21,24]: when exposed to (simulated) body fluids, they form a surface layer of hydroxy-carbonate apatite (HCA) [24]. Natural bone mineral and HCA generated *in vitro* in a simulated body fluid (SBF) feature similar compositions and both comprise small amounts of Na^+ cations substituted in the carbonate-bearing hydroxyapatite [$Ca_5(PO_4)_3OH$] parent lattice. ^{23}Na NMR parameters are reported for bone [25] and synthetic Na-bearing HCA [26], as well as for biomimetic HCA formed *in vitro* by immersing mesoporous bioactive glasses (MBGs) in SBF [27].

Fig. 2a shows the $^{23}Na\{^{31}P\}$ REDOR dephasing curve recorded from an "S90" MBG of nominal composition 10CaO–90SiO_2 after its exposure to SBF for 15 days; this specimen is denoted "S90sbf". It comprises a main Ca-depleted mesoporous silica part (≈90%) and a heterogeneous calcium phosphate layer that mainly constitutes HCA. The observation of a rapid ^{23}Na NMR signal dephasing (only slightly slower than that of Na_3PO_4) unambiguously establishes the incorporation of Na^+ in the HCA structure.

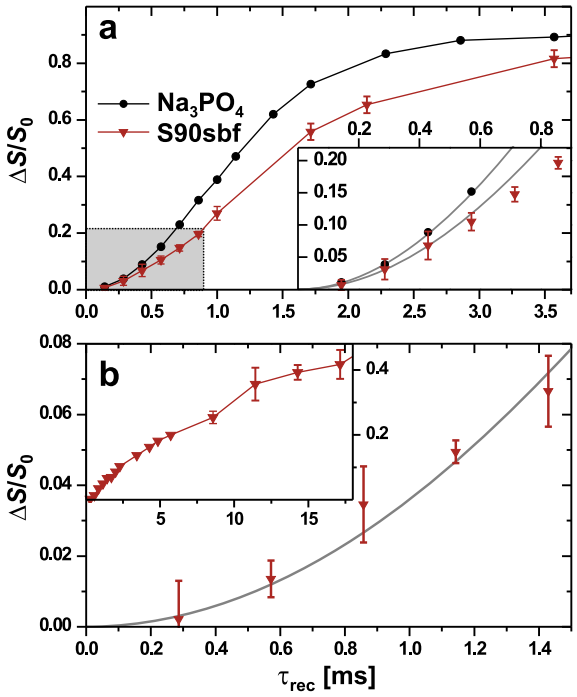

Fig. 2. (a) $^{23}Na\{^{31}P\}$ REDOR and (b) $^{31}P\{^{23}Na\}$ REAPDOR NMR data recorded from the S90sbf sample at B_0 = 9.4 T and MAS rates of (a) 14.0 kHz and (b) 7.0 kHz. The outer graph in (a) includes the dephasing curve from polycrystalline Na_3PO_4 for comparison. The inset displays a zoom of the initial dephasing data (as indicated by the gray area in the outer graph), shown together with best-fit results to Eq. (S1) (gray curve), where only data obeying $\Delta S/S_0 < 0.07$ was included in the fit. (b) Zoom displaying the initial dephasing regime used for fitting to Eq. (S2). Inset: full dephasing curve.

However, its Na content is very low; from elemental analysis it was estimated as one Na^+ species per ≈30 Ca^{2+} cations ($x_{Na}/x_{Ca} \approx 0.03$). The high abundance of PO_4^{3-} groups around each Na site in the HCA component of S90sbf is reflected in the best-fit value $M_2(\text{Na—P}) = (1.00 \pm 0.03) \cdot 10^5\ \text{s}^{-2}$ obtained after using the previously described data correction procedure.

Fig. 2b presents the corresponding $^{31}P\{^{23}Na\}$ REAPDOR NMR results. The minute number of Na^+ ions nearby the PO_4^{3-} groups manifests in a very slow ^{31}P dephasing dynamics. The long-term dipolar dephasing (inset of Fig. 2b) deviates markedly from its expected form, mainly attributed to rf inhomogeneity and a severe sensitivity to even minute MAS-rate fluctuations of the REAPDOR experiment [11,13]. The REDOR NMR curves recorded from the phosphosilicate glasses reveal a similar trend (see Fig. S3 of the SI), although the effects are less prominent relative to those of the present $^{31}P\{^{23}Na\}$ REAPDOR results. Nevertheless, by restricting the data to $\Delta S/S_0 < 0.07$ in the fit to the "universal curve" [20], we obtained the (corrected) dipolar second moment $M_2(\text{P—Na}) = (2.2 \pm 0.3) \cdot 10^4\ \text{s}^{-2}$, which may be contrasted with the REDOR-derived counterpart $M_2(\text{P—Na}) = (2.6 \pm 0.1) \cdot 10^4\ \text{s}^{-2}$ obtained *via* Eq. (2). Both independent estimates accord within 15%, which is a remarkably good agreement in view of the potentially large number of experimental uncertainties involved (including the sample composition).

3. Conclusions

We have demonstrated a straightforward $M_2(\text{S—I}) \leftrightarrow M_2(\text{I—S})$ interconversion [Eq. (2)] to simultaneously determine *both* heteronuclear contacts from a sole recoupling experiment applied to structurally disordered/heterogeneous materials. The procedure was successfully implemented for the {S = ^{31}P, I = ^{23}Na} pair of nuclei in bioactive phosphosilicate glasses. Moreover, we provided (*i*) the first demonstration that REAPDOR NMR data may be analyzed by a straightforward numerical fitting of the initial dephasing regime (without invoking numerical spin-dynamics simulations), analogously to the well-established procedure to derive $M_2(\text{S—I})$ values from REDOR experiments applied to amorphous materials [1]; and (*ii*) the first quantitative assessment of Na ↔ P contacts in Na-bearing biomimetic HCA formed at the surface of a bioactive glass.

Our proposed second-moment conversion strategy is general and independent of both the spin numbers {S, I} involved and the particular heteronuclear recoupling technique employed. It is applicable to a multitude of other S–I pairs, such as ^{27}Al–^{31}P, ^{11}B–^{31}P, ^{11}B–^{29}Si, ^{23}Na–^{29}Si, and ^{27}Al–^{29}Si. However, in the case of S{^{29}Si} experimentation, the advantage of detecting the quadrupolar nucleus $S = \{^{11}B, ^{23}Na, ^{27}Al\}$ for subsequently deriving the $M_2(\text{Si—S})$ result is only realized for ^{29}Si enriched samples. Otherwise, at natural abundance levels of ^{29}Si (≈4.7%), the obvious choice is a ^{29}Si-detected REAPDOR implementation, which unfortunately suffers from low NMR signal sensitivity and the inherent potential dependence of the recoupling on quadrupolar parameters. Note that the $M_2(\text{S—I}) \leftrightarrow M_2(\text{I—S})$ interconversions only operate on the aggregate dipolar second moments. Yet, even in cases where the I-spin NMR spectrum features resolved signals from a set of inequivalent $\{I_j\}$ sites, each associated with a unique $M_2(I_j\text{–S})$ value that is only accessible *via* an independent I{S} recoupling experiment, the net $M_2(\text{I—S})$ result derived from the S{I} counterpart provides an independent constraint of the sum over the individual $M_2(I_j\text{–S})$ values.

Acknowledgements

This work was supported by the Swedish Research Council (contract 2010-4943) and the Faculty of Sciences at Stockholm University. We gratefully acknowledge NMR equipment Grants from the Swedish Research Council, and the Knut and Alice Wallenberg Foundation. We thank Isabel Izquierdo-Barba and María Vallet-Regí (Universidad Complutense de Madrid) for providing the S90sbf specimen.

Appendix A. Supplementary material

Supplementary text and figures associated with this article can be found, in the online version, at http://dx.doi.org/10.1016/j.jmr.2014.12.002.

References

[1] H. Eckert, S. Elbers, J.D. Epping, M. Janssen, M. Kalwei, W. Strojek, U. Voigt, Dipolar solid state NMR approaches towards medium-range structure in oxide glasses, Topics Curr. Chem. 246 (2005) 195–233.
[2] N.C. Nielsen, L.A. Strassø, A.B. Nielsen, Dipolar recoupling, Topics Curr. Chem. 306 (2012) 1–45.
[3] M. Edén, Advances in symmetry-based pulse sequences in magic-angle spinning solid-state NMR, eMagRes 2 (2013) 351–364.
[4] T. Gullion, J. Schaefer, Rotational-echo double-resonance NMR, J. Magn. Reson. 81 (1989) 196–200.
[5] K.T. Mueller, Analytic solutions for the time evolution of dipolar-dephasing NMR signals, J. Magn. Reson., Ser. A 113 (1995) 81–93.
[6] M. Bertmer, H. Eckert, Dephasing of spin echoes by multiple heteronuclear dipolar interactions in rotational echo double resonance NMR experiments, Solid State NMR 15 (1999) 139–152.
[7] J.C.C. Chan, H. Eckert, Dipolar coupling information in multispin systems: application of a compensated REDOR NMR approach to inorganic phosphates, J. Magn. Reson. 147 (2000) 170–178.
[8] W. Strojek, M. Kalwei, H. Eckert, Dipolar NMR strategies for multispin systems involving quadrupolar nuclei: $^{31}P\{^{23}Na\}$ rotational echo double resonance (REDOR) of crystalline sodium phosphates and phosphate glasses, J. Phys. Chem. B 108 (2004) 7061–7073.
[9] J.H. Van Vleck, The dipolar broadening of magnetic resonance lines in crystals, Phys. Rev. Lett. 74 (1948) 1168–1183.
[10] T. Gullion, Measurement of dipolar interactions between spin-1/2 and quadrupolar nuclei by rotational-echo, adiabatic-passage, double-resonance NMR, Chem. Phys. Lett. 246 (1995) 325–330.
[11] T. Gullion, A.J. Vega, Measuring heteronuclear dipolar couplings for I = 1/2, S > 1/2 spin pairs by REDOR and REAPDOR NMR, Prog. NMR Spectrosc. 47 (2005) 123–136.
[12] A. Brinkmann, A.P.M. Kentgens, Sensitivity enhancement and heteronuclear distance measurements in biological ^{17}O solid-state NMR, J. Phys. Chem. B 110 (2006) 16089–16101.
[13] Z. Gan, Rotary resonance echo double resonance for measuring heteronuclear dipolar coupling under MAS, J. Magn. Reson. 183 (2006) 247–253.
[14] Z. Gan, $^{13}C/^{14}N$ heteronuclear multiple-quantum correlation with rotary resonance and REDOR dipolar recoupling, J. Magn. Reson. 184 (2006) 39–43.
[15] S.-J. Huang, S.-B. Liu, J.C.C. Chan, Heteronuclear dipolar recoupling of half-integer quadrupole nuclei under fast magic angle spinning, Solid State NMR 36 (2009) 110–117.
[16] E. Nimerovsky, A. Goldbourt, Efficient rotational echo double resonance recoupling of a spin-1/2 and a quadrupolar spin at high spinning rates and weak irradiation fields, J. Magn. Reson. 206 (2010) 52–58.
[17] E. Nimerovsky, A. Goldbourt, Insights into the spin dynamics of a large anisotropy spin subjected to long-pulse irradiation under a modified REDOR experiment, J. Magn. Reson. 225 (2012) 130–141.
[18] X. Lu, O. Lafon, J. Trébosc, J.-P. Amoureux, Detailed analysis of the S-RESPDOR solid-state NMR method for inter-nuclear distance measurement between spin-1/2 and quadrupolar nuclei, J. Magn. Reson. 215 (2012) 34–49.
[19] A. Goldbourt, S. Vega, T. Gullion, A.J. Vega, Interatomic distance measurement in solid-state NMR between a spin-1/2 and a spin-5/2 using a universal REAPDOR curve, J. Am. Chem. Soc. 125 (2003) 11194–11195.
[20] E. Nimerovsky, A. Goldbourt, Distance measurements between boron and carbon at natural abundance using magic angle spinning REAPDOR NMR and a universal curve, Phys. Chem. Chem. Phys. 14 (2012) 13437–13443.
[21] R. Mathew, B. Stevensson, A. Tilocca, M. Edén, Toward a rational design of bioactive glasses with optimal structural features: composition–structure correlations unveiled by solid-state NMR and MD simulations, J. Phys. Chem. B 118 (2014) 833–844.
[22] B. Stevensson, R. Mathew, M. Edén, Assessing the phosphate distribution in bioactive phosphosilicate glasses by ^{31}P solid-state NMR and MD simulations, J. Phys. Chem. B 118 (2014) 8863–8876.
[23] K. Nishimura, R. Fu, T.A. Cross, The effect of rf inhomogeneity on heteronuclear dipolar recoupling in solid state NMR: Practical performance of SFAM and REDOR, J. Magn. Reson. 152 (2001) 227–233.
[24] L.L. Hench, Bioceramics: from concept to clinic, J. Am. Ceram. Soc. 74 (1991) 1487–1510.
[25] D. Laurencin, A. Wong, W. Chrzanowski, J.C. Knowles, D. Qiu, D.M. Pickup, R.J. Newport, Z. Gan, M.J. Duer, M.E. Smith, Probing the calcium and sodium local

environment in bones and teeth using multinuclear solid state NMR and X-ray absorption spectroscopy, Phys. Chem. Chem. Phys. 12 (2010) 1081–1091.

[26] H.E. Mason, A. Kozlowski, B.L. Phillips, Solid-state NMR study of the role of H and Na in AB-type carbonate hydroxylapatite, Chem. Mater. 20 (2008) 294–302.

[27] P.N. Gunawidjaja, A.Y.H. Lo, I. Izquierdo-Barba, A. García, D. Arcos, B. Stevensson, J. Grins, M. Vallet-Regí, M. Edén, Biomimetic apatite mineralization mechanisms of mesoporous bioactive glasses as probed by multinuclear ^{31}P, ^{29}Si, ^{23}Na and ^{13}C solid state NMR, J. Phys. Chem. C 114 (2010) 19345–19356.